Viscoelastic Properties and Collapse Behavior of a Smectic Liquid-Crystalline Polymer at the Air/Water Interface

Jörg Adams, Alexander Buske, and Randolph S. Duran*

Center for Macromolecular Science and Engineering, Department of Chemistry, University of Florida, Gainesville, Florida 32611

Received October 6, 1992

ABSTRACT: The viscoelastic behavior of a monolayer of a liquid-crystalline side-chain polymer in its collapse region is discussed. The material shows a reversible collapse with a strong temperature and compression speed dependence. The collapse process can be empirically described as a viscoelastic relaxation with two relaxation times. Because of this behavior, the importance of the "time of observation" is pointed out. A second increase of the surface pressure at lower mean molecular area and stepwise increases of the collapse viscosity are associated with the formation of bi- and trilayers. Reflectivity measurements with a Brewster angle microscope are used to confirm that the collapse is a homogeneous process, leading to multilayers with liquid crystalline properties at the air/water interface.

Introduction

In two recent papers, Kato and co-workers[1,2] described the importance of the *time of observation* when interpreting the surface pressure (π) versus surface area (Å^2) isotherm of monolayers at the air/water interface. The conclusion which can be drawn from this work is that time-dependent processes play an important role during the compression of a monomolecular film. The usually discussed properties like film stability, collapse pressure, and compressibility[3] give for most insoluble films only a momentary picture of the film characteristics. However, the complete properties are determined not only by factors such as temperature, subphase composition, or spreading solvent but also by the time that was given to the molecules to pack in their lowest energy conformation.

This is especially true for monolayers formed from polymers spread from solution. Compared with low molecular weight amphiphiles, surface active polymers are known not only for their superior monolayer and multilayer properties, such as mechanical and thermal stability[4–7] but also for strongly time-dependent behavior in the bulk phase.[8] While most polymer researchers keep the time dependence of their observation in mind, many scientists working on Langmuir films do not.

In this paper we discuss the influence of time on the behavior of a monolayer of a side-chain polymer which forms smectic liquid-crystalline phases in the bulk. The influence of the chemical structure of this material, its transfer behavior to solid substrates, and investigations of its ferroelectric switching behavior is presented elsewhere.[9–13]

Here we will discuss primarily the film behavior during and after the collapse. This region of the isotherm, which is often treated as being irreproducible, is a valuable source of information about the structure of the monolayer at the air/water interface as well as the multilayers that can be prepared from it.

That the collapse region of a liquid crystal can be of great interest has been shown by Diep-Quang and Ueberreiter[14] and Rapp et al.[15,16] For a low molecular weight smectic liquid crystal (LC), peaks in the isotherm were observed on compressing beyond the collapse point.[15] These peaks occurred at areas in the relation $1:{}^1/_2:{}^1/_3$ and were interpreted as first-order transitions, caused by a stepwise formation of smectic layers.

So far, this collapse to smectic multilayers at a liquid interface has not been reported for a LC polymer. One reason for this might be the time of observation, which is generally longer for a polymeric LC, because of its slower response to changes of pressure, area, and temperature.

In this publication, relaxations of Langmuir films of a liquid crystalline polymer above and below its collapse region are considered. Together with relaxation measurements, Brewster angle reflectivity is used to describe the collapse region.

Experimental Section

The chemical structure of the liquid crystalline polymer, 8PPB2-CO, is shown in Figure 1 together with its thermal bulk phase behavior. The synthesis is described elsewhere.[17] It was purified by several reprecipitations from a tetrahydrofuran solution into methanol.

For monolayer experiments, 8PPB2-CO was dissolved in chloroform (Fisher, spectranalyzed grade). The concentrations ranged from 0.5 to 2.5 mg/mL.

The experiments were carried out on a commercially available Langmuir trough LB5000 (KSV-Instruments Inc., Finland) with computerized control and either one or two barriers. A Wilhelmy balance was used as a surface pressure sensor. The trough material is poly(tetrafluoroethylene) (PTFE), the barriers were made from Nylon or PTFE. Purified water (Millipore, ≥18 MΩ resistance) was used as the subphase. Reported temperatures refer to the subphase temperature.

All isotherms and hysteresis experiments were performed with a constant barrier speed, expressed in Å^2/(mesogenic repeat unit)/min unless otherwise noted in the text. In hysteresis experiments, the barrier movement was immediately reversed after the area reached the desired value.

Because a constant barrier speed was used rather than a constant strain rate, the reader should keep in mind that the "time of observation", which is defined as the reciprocal of the strain rate,[1,2] is not constant in this work over the entire experiment but decreases with decreasing area. The use of a constant strain rate was not possible due to the experimental conditions.

The reflectivity of the monolayer was obtained with the help of a BAM-1 Brewster angle microscope (Nanofilm Technologie) interfaced to a SUN Sparc Station. The incident laser was set to the Brewster angle of water (53°) with the polarization set parallel to the plane of incidence (p-polarization). A rotatable polarizer could be positioned in the reflected beam to get information about birefringent regions in the monolayer. The reflectivity was then calculated from the microscope images by integration of the light intensity over the field of view with the help of image processing software (VideoPix, SUN Microsystems Inc., 640 × 480 pixels in 256 gray levels). Further details of the Brewster angle microscopy technique can be found elsewhere.[18–20]

0024-9297/93/2226-2871$04.00/0

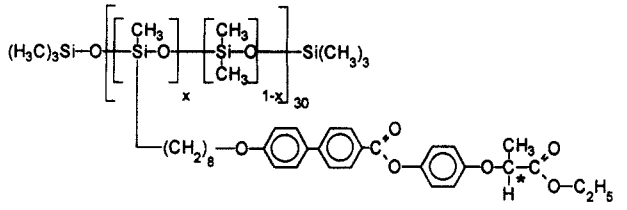

Figure 1. Chemical structure and thermal properties (by DSC) of 8PPB2-CO. T_g, glass transition; S, smectic phase; iso, isotropic phase.

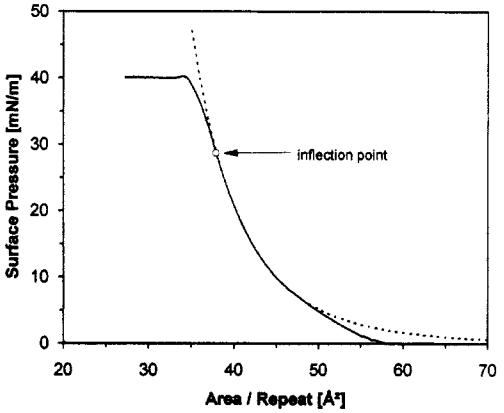

Figure 2. (—) Isotherm of 8PPB2-CO at 27 °C with 4.2 Å²/repeat/min. (- - -) Fit of 8PPB2-CO with eq 1 and $\nu = 0.596$.

Results and Discussion

Monolayer Structure and Orientation. Even though 8PPB2-CO contains none of the commonly used hydrophilic groups like carboxylic acid, alcohol, or PEO units, well-behaved monolayers could be spread from chloroform solutions as shown in the surface pressure/surface area per repeat unit (ARU) isotherm of Figure 2.

We define a repeat unit as the mesogenic side chain including its methylsiloxane unit, plus the dimethylsiloxane units of the comonomer ($\{xM_{\text{side chain}} + (1 - x)M_{\text{PDMS}}\}x^{-1}$; $x = 0.3$).

As shown in Figure 2 the pressure onset at the beginning of this isotherm occurs at about 57 Å²/repeat and collapse occurs for this particular compression speed at 40 mN/m. The slopes indicate a highly compressible film. That the copolymer behaves as a typical polymer can be seen by the fit (dotted line) that is also plotted in Figure 2. The pressure π in this fit is calculated according to the scaling law[21-23] by

$$\pi \sim C^y \tag{1}$$

$$y = 2\nu/(2\nu - 1), \quad \pi = \gamma_0 - \gamma \tag{2}$$

with C as the concentration of the repeat units per area and ν as a characteristic scaling exponent. γ_0 and γ are the surface tensions of the water surface before and after adding the surface-active polymer, respectively. The parameter ν expresses the dependence of the radius of gyration of the polymer on its molecular weight for a given solvent or, as in this case, gas/liquid interface. For a good solvent the exponent ν is calculated to be 0.77, and for a Θ solvent $\nu = 0.505$.[24,25] The experimental value for 8PPB2-CO is $\nu = 0.596$ which implies that the polymer at a water interface behaves nearly as though in a Θ solvent. It should be noted that the mesogenic side chain alone behaves considerably differently and the scaling expression of eq 1 cannot be fit to its isotherm.[11]

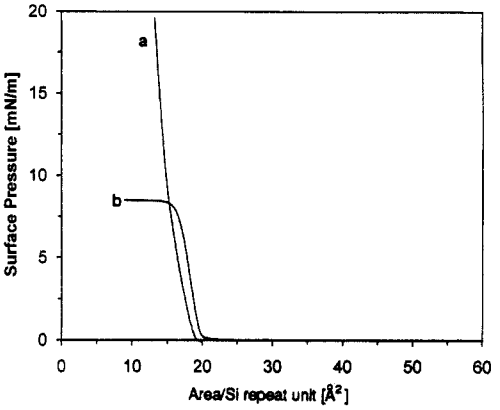

Figure 3. Comparison of PDMS and 8PPB2-CO isotherms: (a) 8PPB2-CO; (b) PDMS (M_w = 55 000).

In Figure 2, the experimental isotherm and calculated curve deviate from each other at low surface pressures and high areas. This can be attributed to two factors. First, at high surface areas, fluid domains of the polymer separated by regions of pure water can be seen by the Brewster angle microscope.[9] This shows that the polymer chains do not tend to spread and form a gas analogous phase with isolated single polymer chains. Thus the scaling expression would not be expected to hold at low pressures. Second, at low pressures, an additional factor may influence the observed scaling law fit: the structure and thus the surface tension of the water (γ_0) in the vicinity of the polymer may be changed by hydration forces.

At high pressures, the experimental and calculated curves start to deviate at the inflection point of the experimental curve. This can be associated with the onset of the collapse process as will be discussed in more detail below.

Compared to a corresponding homopolymer and the monomeric side chain, the area per repeat unit at the onset is strongly shifted to higher values,[9-12] when a repeat unit is considered as the side chain plus 2.3 repeat units. However, when considering all the siloxane units as repeat units (i.e., $x = M_{\text{side chain}} + (1 - x)M_{\text{PDMS}}$), the onset area is lowered to ca. 20 Å²/repeat, a value which is close to the onset area of pure PDMS.[26,27] Figure 3 shows a comparison of these isotherms.

The small difference between the two onset areas may be in part due to small discrepancies in the degree of substitution of the copolymer. A value of 30 is used, based on manufacturer's specifications of the siloxane intermediate; the value measured by ^{1}H NMR for a similar polymer was slightly higher.

Nonetheless, the similarity of the areas leads us to assume that the isotherm is, at least at low pressures, mainly dominated by the PDMS backbone. The siloxane backbone in the copolymer studied here is in contact with the water surface, having its oxygen atoms pointing toward the water, as has been already observed for pure PDMS.[26,27] Due to the packing of the polymer backbone and their low substitution density, the mesogens cannot get close enough to each other to be close packed normal to the plane of the monolayer and must assume a tilted conformation.

Hysteresis. When the monolayer is compressed far into the collapsed region and expanded again, hysteresis curves as shown in Figure 4 for three different compression speeds are obtained.

The zero speed curve (c) was obtained by a stepwise compression of the monolayer to a desired area, followed

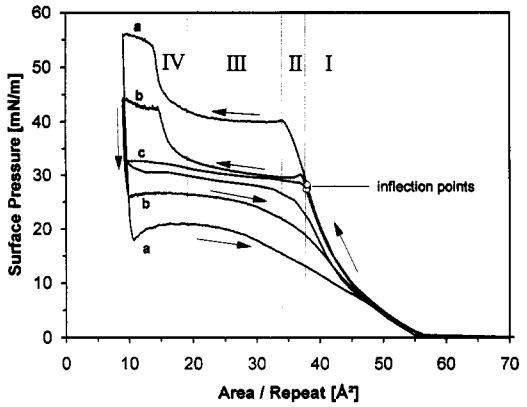

Figure 4. Hysteresis of 8PPB2-CO at 27 °C for different compression speeds: (a) 4.2, (b) 0.34, (c) 0 Å²/min.

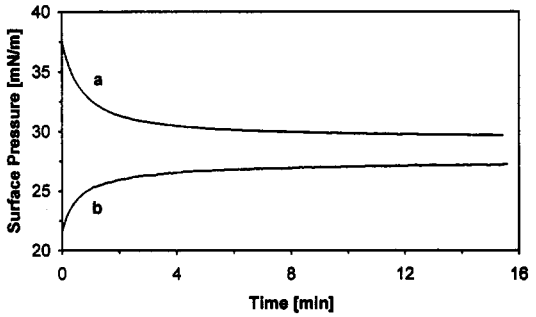

Figure 5. Relaxation of the surface pressure after compression/expansion at constant surface area: (a) after compression to 30 Å²; (b) after expansion to 28 Å². Temperature 25 °C; compression/expansion speed 4.2 Å²/(repeat unit)/min.

by the relaxation of the pressure to a constant value. This value is then plotted against the area per mesogenic repeat unit in Figure 4c. The manner in which the surface pressure relaxes in this region is shown in Figure 5. The surface pressure after compression decreases, whereas on expansion it increases as soon as the barriers stop moving.

The hysteresis curves in Figure 4 are interpreted as follows: the first part (region I) of the isotherms, up to the inflection point, is independent of the compression speed. This means that the relaxation processes, which take place while the molecules are compressed, are too fast to be seen even with the highest speed, or, in other words, the time of observation is longer than the relaxation time of the involved physical process.

After the inflection point (region II) no correspondence of the three curves can be observed. The higher the speed, the further the monolayer can be compressed before leveling off to a plateau between 40 and 20 Å². While for the highest speed, a pressure of 40 mN/m is reached before the monolayer conspicuously collapses, at 0.34 Å²/min collapse occurs already at 30 mN/m and for 0 Å²/min immediately after the inflection point (28.6 mN/m). This means that the part of the isotherm above the inflection point is only a product of the applied barrier speed and only curve c describes properties independent of the experimental conditions.

The surface pressure in this region is not only the difference of the surface tension of the water surface and the film covered surface. Also a term considering the viscoelastic pressure in the monolayer has to be added, including the fact that the film cannot relax as fast as it gets compressed and therefore builds up an internal stress.

Interpreting this behavior again with the concept of time of observation, the processes in the monolayer have changed and the times of observation are now of the same order of magnitude as the relaxation time of these processes.

In the collapse plateau the surface pressure for all three curves increases in linear fashion (region III). Because it increases even for the equilibrium curve, we believe that the equilibrium pressure is not equal to the equilibrium spreading pressure (ESP) of liquid and solid materials which can be spread on a liquid/air interface from the bulk.[3] For such materials an equilibrium exists between the bulk crystal or liquid droplet and the monolayer. If the area is decreased, molecules from the monolayer can migrate into the three-dimensional phase, leaving the surface pressure constant and the structure of the monolayer unchanged. Because the surface pressure is not constant with decreasing surface area in 8PPB2-CO, the steady increase of the pressure is a first indication that the monolayer is constantly and homogeneously collapsing in region III. In other words, the slope of the curve in this region is an indication of the change in surface tension between the monolayer and the bilayer, which is expected to be small compared to the surface tension of the water surface and the monolayer.

In region IV curves a and b in Figure 4 show a second increase in the surface pressure, which levels at ~15 Å²/repeat unit into a second plateau. We associate this with the formation of a bilayer as has been observed for low molecular weight smectic LCs.[15] In region IV the bilayer becomes close-packed and therefore changes the film properties. However, the equilibrium pressure does not show this increase, as can be seen from Figure 4b. The same considerations that were used to explain region II can be used again to explain why the pressure increases during compression and why it remains unchanged for the equilibrium curve.

The plateau in region IV is associated with the formation of a trilayer. The close packing of the trilayer cannot be observed in these curves, because the compression speeds of curves a and b in Figure 4 are both too high. Creep experiments, as discussed later, are able to show the buildup of the third and the fourth layer.

On expansion, the sequence of the speed dependence is reversed. The higher the expansion speed, the lower the measured pressure and the larger the hysteresis. The small hysteresis observed for curve c in Figure 4 is mainly due to water evaporation, because the whole experiment lasted 20 h.

All curves merge with the initial compression curves at high areas. The collapse is a reversible collapse which can be reproduced with the same monolayer several times (see below).

Temperature Dependence. As can be expected for a monolayer with pronounced viscoelastic properties,[28] a strong temperature dependence can also be observed (Figure 6). Increasing the temperature shifts the isotherm to only slightly higher areas/repeat unit (i.e., low expansion coefficient of the monolayer) but lowers the collapse pressure for this particular compression speed drastically. This effect can be seen in Figure 6b, where the pressures at 23 Å² and of the inflection points are plotted versus the temperature.

The negative $(\Delta\pi/\Delta T)$ for both pressures indicates that the collapse is kinetically and not thermodynamically controlled, like a phase transition from, for example, a liquid expanded to a condensed phase.

Relaxation. As mentioned earlier, the dynamic surface pressure during compression (expansion) decreases (increases) to the equilibrium pressure after the barriers are stopped in the collapse region. To get information on

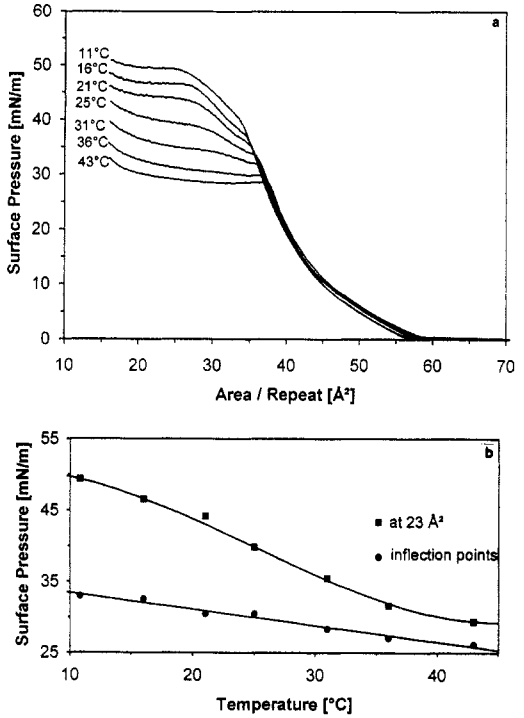

Figure 6. Temperature dependence of 8PPB2-CO: (a) isotherms; (b) surface pressure of the inflection point and at 23 Å²/repeat unit. Compression speed 4.2 Å²/(repeat unit)/min.

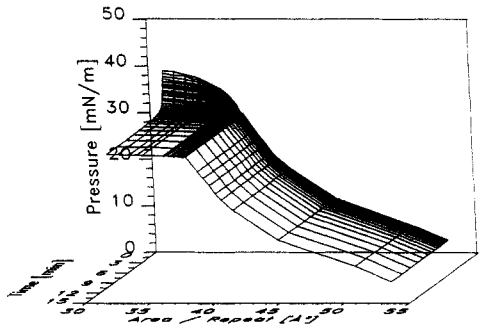

Figure 7. Surface pressure of 8PPB2-CO versus of the area/repeat unit and time. Temperature 25 °C; compression speed 10 Å²/(repeat unit)/min.

how this relaxation develops from the stable part of the isotherm into the collapse region, relaxation measurements were performed at different temperatures and compression speeds. The experiments were performed in the same way as for the zero speed isotherm in Figure 4c, except that, after the pressure relaxed to the equilibrium value, the film was expanded completely to ca. 70 Å²/repeat unit and then compressed to the next mean molecular area. This technique assures the same initial conditions for each mean molecular area.

When plotting the pressure versus the surface area and time, a three-dimensional plot can be obtained (Figure 7).

A clear feature of the surface generated is the abrupt change from the stable part of the isotherm to the unstable, collapse region. While the pressure up to 29.4 mN/m remains constant after the barriers are stopped, further compression leads to an exponential decay of the surface pressure like that seen in Figure 5. Below this pressure, the monolayer can be successfully transferred to a solid substrate, resulting in multilayers with unique ferroelectric properties.[12,13,29]

From the pressure relaxation the relaxation time τ for the collapse can be calculated. Attempts to fit the experimental curves with a viscoelastic equation, which has been used successfully to describe phase transitions

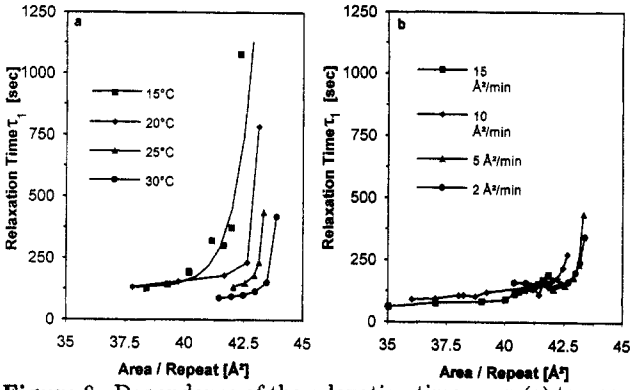

Figure 8. Dependence of the relaxation time τ_1 on (a) temperature at 5 Å²/(repeat unit)/min compression speed and (b) compression speed at 25 °C.

in monolayers,[30,31] failed. However, when assuming that two processes are involved in the collapse, each with its own relaxation time, the relaxation could be described by

$$\pi_t = \pi_\infty + \sum_{i=1}^{2} \pi_{0,i} e^{-t/\tau_i} \tag{3}$$

with π_∞ as the equilibrium surface pressure and $\pi_{0,i}$ as the fraction of the pressure at $t = 0$ associated with the relaxation time τ_i in the way that $\pi_{t=0} = \pi_\infty + \pi_{0,1} + \pi_{0,2}$.

The two relaxation times differed by a factor of about 10. τ_1 is in the range of 54–1100 s, depending on temperature and pressure, whereas τ_2 lies between 8 and 100 s. Because the temperature and compression speed dependences of both parameters are qualitatively similar, only the behavior of τ_1 is shown (Figure 8). It should be noted that a three or more term fit to the observed data was not meaningful in that the coefficients beyond the second term become negligibly small.

As Figure 8a shows, temperature has a strong influence on the relaxation times, which is especially evident at the beginning of the collapse process at the highest areas, i.e., lowest pressures. The compression speed has almost no effect on the relaxation time (Figure 8b).

This is reasonable, because a kinetically controlled collapse should be temperature dependent but not speed dependent. The molecules in the monolayer have to overcome an energy barrier, E_a, in order to move from the water interface into the bilayer. An increase in temperature should therefore increase the collapse rate (i.e., decrease the relaxation time). The change in compression speed only affects how far the system is driven away from equilibrium. This is reflected in an increase in $\pi_{0,i}$ with increasing speed and not in τ.

So far it is not clear what causes the appearance of two relaxation times instead of only one. We do not believe that the Marangoni effect plays a part in the relaxation. The Marangoni effect causes a change in the surface pressure due to water that is dragged by the monolayer during the compression.[32,33] This relaxation has a relaxation time of only a few seconds and can, therefore, not explain the maximum τ-values we observed. Interpretation in terms of different components of an anisotropic viscosity tensor may be valuable,[34] but further measurements are necessary to do this in a meaningful manner.

The different mobility of the side-chain and the polymer might provide a better explanation. We can, for instance, associate the fast process with the movement of single side-chain segments, whereas the slow relaxation is associated with the rearrangement of the polymer backbone chain including several mesogenic groups.

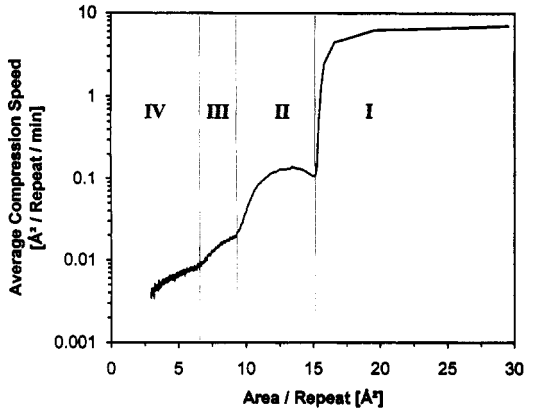

Figure 9. Compression speed in the collapse region at 45 mN/m and 27 °C. The roman numbers indicate regions of multilayer formation: (I) bilayer; (II) trilayer; (III) quadruple layer; (IV) quintuple layer.

Attempts to calculate relaxation times for the second pressure increase at low areas failed, probably because the process is too complicated to be described with a simple model like eq 3. This can be understood when considering that a molecule at the water surface now has to move through the second layer to get into the new third layer. This more complex behavior has also been observed for the low molecular weight LCs in the investigations of Rapp and Gruler.[15]

Bilayer Formation. As already mentioned, only the formation of the condensed bilayer can be seen in normal isotherms at constant compression speed. To better resolve the formation of the bilayer and multilayer, the collapse velocity at constant pressure was measured.

In this experiment, which is identical to creep experiments to determine the monolayer stability, the surface pressure was set to a value above the pressure of the inflection point of the isotherm. The compression speed required to maintain this surface pressure is then recorded and plotted on a logarithmic scale versus the area/repeat unit in Figure 9.

This experimental procedure has the advantage that the time of observation is controlled by processes in the Langmuir film and not by preset experimental conditions such as compression speed or compression rate.[2] A wider spectrum of relaxation times can be covered because the time of observation (i.e., compression speed) changes automatically if the relaxation time changes. In Figure 9 a time spectrum of 4 orders of magnitude is covered for the compression speed in an experiment that lasted 14 h.

At the beginning of the experiment in region I the compression speed has its highest value of 10 Å²/(repeat unit)/min. As soon as the bilayer starts to get close packed, the speed drops rapidly to a minimum of 0.1 Å²/min at 15 Å². This is followed by a short increase and a further decline (region II).

These observed changes in the rate can be understood as follows. When just a monolayer is present, segments at the air/water interface can easily be pushed up and form a bilayer. Once a bilayer is formed, segments at the air/water interface must be pushed up two layers to form a trilayer, which is a much slower process. A still slower process would be expected in forming a quadruple layer from the trilayer.

The minimum at the transition from region I to II can be explained by the nucleation and growth process of the collapse. The bilayer is metastable compared to the trilayer because defects which are necessary to move molecules from the bilayer into the trilayer are not present in sufficient number. The metastable region is also seen as a small peak in the isotherm when the film is compressed past the inflection point at low compression speed (Figure 4b). Similar behavior has been observed by Rapp.[15,16]

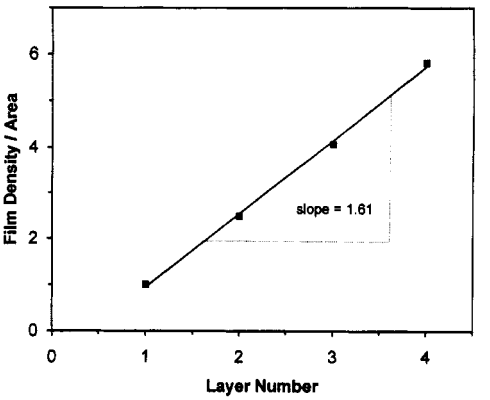

Figure 10. Inverse ratios of the areas/repeat unit for the multilayers versus the layer number.

No minima can be seen when the area decreases further, but at 9.3 and 6.5 Å² a pronounced change in the slope of the compression speed occurs. Assuming these as the points where a trilayer and quadruple layer get close packed and using the inflection point at 37.7 Å²/repeat unit as the area of the close-packed monolayer, a relation of $1:{}^{1}/_{2.5}:{}^{1}/_{4.1}:{}^{1}/_{5.8}$ for the areas is calculated.

The ratios do not follow the expected relation of $1:{}^{1}/_{2}:{}^{1}/_{3}:{}^{1}/_{4}$, etc., for the collapse into a multilayer with the same structure and density as the monolayer they were built from. However, assuming that the whole collapse and the buildup of multilayers are induced by the liquid crystalline character of the copolymer and considering that the area per repeat unit of 8PPB2-CO is higher than the areas of the corresponding LC monomer and homopolymer,[9-12] a reasonable model able to explain the observations can be proposed. The ARU of the monolayer at the water interface is in part determined by the interaction with the water. When the monolayer collapses, this interaction is lost for the molecules that are pushed away from the interface into the bilayer. These molecules start to build a new layer due to the liquid crystalline nature of the polymer. However, the density of a close-packed LC layer is higher, and therefore the bilayer will only get close packed at an area less than half of the monolayer collapse area.

That this model is reasonable can be seen in Figure 10. Plotted is the inverse of the area ratios of the different layers versus the layer number. The inverse of the ratios corresponds to the concentration of repeat units per area, normalized by the concentration of the monolayer at the inflection point.

A linear relationship is obtained with a slope of 1.61. The slope represents the factor by which the concentration of the monolayer has to be multiplied to give the concentration per repeat units in each consecutive layer. From this the ARU in the multilayer is calculated to be 23.4 Å². This value is comparable with the collapse area of 24.5 Å² measured for the homopolymer 10PPB2P which has the same mesogenic side chain except for an alkyl spacer of 10 instead of 8 methylene units.

This comparison of the homopolymer and the copolymer gives only a crude estimate of the ARU calculated for the multilayers. The problem is that the surface pressure is a property of both the water interface and the spread molecule. The molecules in the multilayer, with the exception of the first, are not at this interface and therefore experience a different pressure.

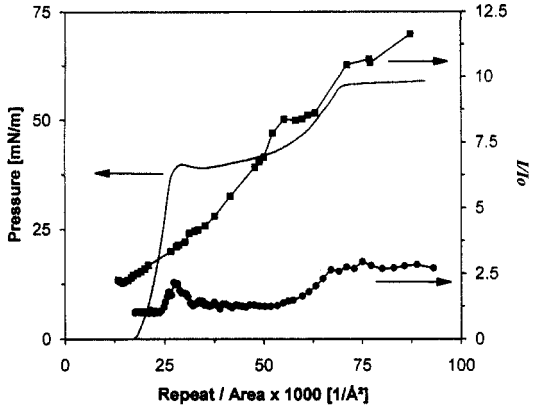

Figure 11. Relative Brewster angle microscope reflectivity of 8PPB2-CO and surface pressure versus concentration of repeat units per area: (■) without polarizer in the reflected beam; (●) polarizer in the reflected beam, 90° to the polarization of the emitted light. Compression speed 5 Å²/(repeat unit)/min; temperature 25 °C.

Due to this different pressure, the density of the multilayer is closer to the density of the bulk material. Density measurements of the bulk would therefore be helpful to get more information about the structure of the multilayers. X-ray investigations on Langmuir–Blodgett films of the copolymer 10PPB2-CO have shown that the density of the monolayer is lower than the density of the LB multilayer.[35]

With the Brewster angle microscope,[18-20] structural changes of the monolayer and the bilayer were observed. The monolayer forms a liquid expanded film with separate domains at high areas.[9] These domains flow together to form a homogeneous film which remains featureless over the whole compression range.

The reflection intensity of the images increases while the area decreases and small birefringent grains appear as soon as the monolayer gets condensed when the monolayer is viewed under crossed polarizers. The birefringence is attributed to domains where the mesogenic side chains are aligned all in the same direction due to long-range orientational interactions. These liquid crystalline domains do not grow on annealing because of the disorder and viscosity of the polymer backbone.

When integrating the intensity of the reflected light over the field of view, the relative reflectivity $R = I/I_0$ can be calculated. I is the intensity of the monolayer at a specific area, I_0 is the intensity of the pure water surface. In Figure 11 the reflectivity of the Langmuir film with crossed polarizers and without polarizer in the pathway of the reflected beam is shown together with the surface pressure.

The reflectivity without polarizer shows a constant increase over the whole compression range, indicating that the collapse process is homogeneous and the film is constantly changing thickness.

The reflectivity with crossed polarizers gives information about structural features. When the surface pressure starts to increase, a peak in the reflectivity can be observed, and when the bilayer gets close packed, R increases again. The peak in R overlaps with the metastable region of the monolayer discussed above. Our interpretation is that the mesogens in the metastable monolayer get close enough to form liquid crystalline domains. After the metastable region the density can decrease due to the relaxation process and therefore the domains become less birefringent.

Molecules that are transferred from the monolayer into the bilayer give no contribution to the birefringence although a steady increase of the reflectivity without polarizer is observed. This implies that for the long-range orientational order a minimum density is necessary.

At the second onset of the surface pressure the birefringence increases again because a more dense liquid crystalline-like bilayer is formed. Further compression leads to an almost constant reflectivity.

The formation of the trilayer cannot be seen because the experimental conditions did not allow us to compress to sufficiently low areas.

Conclusions

This work has shown the relaxation and ordering behavior of a side-chain copolymer in the monolayer collapse region. The monolayer's surface pressure is shown to be temporally stable at areas larger than the inflection point of the surface pressure isotherm and depends on packing of the polymer backbone at low pressures.

At pressures above the isotherm inflection point, the monolayer collapses to form a partially bilayer system. The pressure relaxation corresponding to the collapse is found to fit to a two-term exponential equation with relaxation times which were strongly temperature dependent. The relaxation behavior changed substantially upon the close-packed bilayer and the onset of trilayer formation. Bilayer and trilayer formation were also probed by Brewster angle microscopy and isobaric collapse velocity experiments. These showed that, while birefringence increased at the close-packed monolayer and bilayer, the collapse process appeared to be homogeneous.

Relaxation experiments of polymers in restricted geometries like these may provide valuable information on the approach of tethered polymers toward bulk behavior.

Acknowledgment. We thank Prof. R. Shashidhar of Geo Centers Inc. and Dr. J. Naciri of NRL for donating the polymer samples used in this study. Technical assistance from KSV Instruments, Helsinki, Finland, and Nanofilm Technologie, Göttingen, Germany, is gratefully acknowledged. We also acknowledge partial support from NSF Grant No. DMR9113550, Deutsche Forschungs Gemeinschaft, and the Center For Bio-Molecular Science and Engineering at NRL.

References and Notes

(1) Kato, T. *Langmuir* **1990**, *6*, 870.
(2) Kato, T.; Hirobe, Y.; Kato, M. *Langmuir* **1991**, *7*, 2208.
(3) Gaines, G. L. *Insoluble Monolayers at Liquid–Gas Interfaces*; John Wiley & Sons: New York, 1966.
(4) Winter, C. S.; Tredgold, R. H.; Vickers, A. J.; Khoshdel, E.; Hodge, P. *Thin Solid Films* **1985**, *134*, 49.
(5) Lupo, D.; Prass, W.; Scheunemann, U. *Thin Solid Films* **1989**, *178*, 403.
(6) Erdelen, C.; Laschewsky, A.; Ringsdorf, H.; Schneider, J.; Schuster, A. *Thin Solid Films* **1989**, *180*, 153.
(7) Matzenbach, A.; Ottenbreit, P.; Prass, W. *Makromol. Chem., Macromol. Symp.* **1991**, *46*, 353.
(8) Scherer, G. W. *Relaxation in Glass and Composites*; John Wiley & Sons: New York, 1986.
(9) Adams, J.; Rettig, W.; Naciri, J.; Shashidhar, R.; Duran, R. S. *J. Phys. Chem.* **1993**, *97*, 2021.
(10) Rettig, W.; Naciri, J.; Shashidhar, R.; Duran, R. S. *Macromolecules* **1991**, *24*, 6539.
(11) Rettig, W.; Naciri, J.; Shashidhar, R.; Duran, R. S. *Thin Solid Films* **1992**, *210*, 114.
(12) Thibodeaux, A.; Adams, J.; Duran, R. S., in preparation.
(13) Pfeiffer, S.; Adams, J.; Duran, R. S.; Shashidhar, R., submitted for publication in *Appl. Phys. Lett.*
(14) Diep-Quang, H.; Ueberreiter, K. *Polym. J.* **1981**, *13*, 623.
(15) Rapp, B.; Gruler, H. *Phys. Rev. A* **1990**, *42*, 2215.
(16) Rapp, B.; Eberhardt, M.; Gruler, H. *Makromol. Chem., Macromol. Symp.* **1990**, *46*, 439.

(17) Naciri, J.; Pfeiffer, S.; Shashidhar, R., submitted for publication in *Liq. Cryst.*
(18) Hoenig, D.; Moebius, D. *J. Phys. Chem.* **1991**, *95*, 4590.
(19) Henon, S.; Meunier, J. *Rev. Sci. Instrum.* **1991**, *62*, 936.
(20) Hoenig, D.; Overbeck, G. A.; Moebius, D. *Adv. Mater.* **1992**, *4*, 419.
(21) de Gennes, P.-G. *Scaling Concepts in Polymer Physics*; Cornell University Press: Ithaca, NY, 1979.
(22) Doud, M.; Cotton, J. P.; Franoux, B.; Jannink, G.; Sarma, G.; Benoit, H.; Duplessix, R.; Picot, C.; de Gennes, P.-G. *Macromolecules* **1975**, *8*, 804.
(23) Vilanove, R.; Rondelez, F. *Phys. Rev. Lett.* **1980**, *45*, 1502.
(24) Le Guillou, J. C.; Zinn-Justin, J. *J. Phys. Rev. Lett.* **1977**, *39*, 95.
(25) Stephen, M.; McCauley, J. *J. Phys. Rev. A* **1973**, *44A*, 89.
(26) Noll, W.; Steinbach, H.; Sucker, Chr. *J. Polym. Sci., Part C* **1971**, *34*, 123.
(27) Kalachev, A. A.; Litvinov, V. M.; Wegner, G. *Makromol. Chem., Macromol. Symp.* **1991**, *46*, 365.
(28) Yoo, K. W.; Yu, H. *Macromolecules* **1989**, *22*, 4019.
(29) Adams, J.; Thibodeaux, A.; Naciri, J.; Shashidhar, R.; Duran, R. S. *Polym. Prepr. (Am. Chem. Soc., Div. Polym. Chem.)* **1992**, *33*, 1164.
(30) Bois, A. G.; Panaiotov, I. I.; Baret, J. F. *Chem. Phys. Lipids* **1984**, *34*, 265.
(31) Bois, A. G.; Baret, J. F.; Kulkarni, V. S.; Panaiotov, I. I.; Ivanova, M. G. *Langmuir* **1988**, *4*, 1358.
(32) Dimitrov, D. S.; Panaiotov, I. I. *Ann. Univ. Sofia, Fac. Chim.* **1975/76**, *70*, 103.
(33) Dimitrov, D. S.; Panaiotov, I. I.; Richmond, P.; Ter-Minassian-Sarga, L. *J. Colloid Interface Sci.* **1978**, *65*, 483.
(34) Kawaguchi, M.; Sauer, B.; Yu, H. *Macromolecules* **1989**, *22*, 1735.
(35) Geer, B.; Thibodeaux, A.; Duran, R. S.; Shashidhar, R., to be published in *J. Phys. Lett (Paris)*.